JOURNAL OF Materials CHEMISTRY

New intercalation compounds for lithium batteries: layered $LiMnO_2$†

Peter G. Bruce,* A. Robert Armstrong and Robert L. Gitzendanner

School of Chemistry, University of St. Andrews, St. Andrews, Fife, UK KY16 9ST

Received 27th March 1998, Accepted 26th May 1998

The mechanism of lithium intercalation in layered $LiMnO_2$ has been investigated by combining data from a variety of techniques, including powder X-ray and neutron diffraction, cyclic voltammetry and galvanostatic cycling. Whereas the diffraction data indicate the coexistence of layered and spinel phases at $Li_{0.5}MnO_2$ after 5 charge(extraction)–discharge(insertion) cycles, the electrochemical data only change significantly on the first charge(extraction), near $Li_{0.5}MnO_2$. A rationale is provided by a model in which, on first extracting 0.5 Li from layered $LiMnO_2$, displacement of Mn ions occurs into the lithium layers, forming regions with the local structure and composition of spinel. This can explain the presence of a 4 V peak in the cyclic voltammogram on the first charge. Long range order only develops on more extended cycling and since this does not alter significantly the Li^+ or e^- energies, the electrochemistry does not change further. Load curves show significant hysteresis and this is linked to a domain-like microstructure with spinel imbedded in layered material. The marked difference between load curves for this material and $LiMn_2O_4$ spinel indicates that the former does not convert to 'normal' spinel on cycling. By doping $LiMnO_2$ with as little as 10% Co the cooperative Jahn–Teller distortion due to localised high spin $Mn^{3+}(3d^4)$ disappears despite the high concentration of Mn^{3+} and a substantial improvement in the ability to cycle lithium is obtained from 130 mAh g^{-1} to 200 mAh g^{-1} at 100 μA cm^{-2}.

Introduction

The synthesis of new compounds is a cornerstone of solid state chemistry. There are two powerful motivating forces which drive such syntheses of new solids. The first is our curiosity to prepare solids with new compositions and new or unusual structures and the second is technology. The latter is often a more demanding discipline than the former as illustrated by the contents of Table 1, in which the requirements that must be satisfied by an intercalation solid if it is to be successful as a positive electrode in rechargeable lithium batteries are presented. We shall return to these requirements later but it is evident that designing and then synthesising a material which possesses so many diverse attributes is indeed a significant challenge, demonstrating that it is, in many senses, easier to be interesting than to be useful.

Rechargeable lithium batteries now represent a major industrial activity with production in 1997 alone exceeding 200 million and doubling each year! A schematic representation of a rechargeable lithium battery is shown in Fig. 1. The cell consists of two intercalation compounds separated by a liquid electrolyte.[1,2] One intercalation solid, $LiCoO_2$, acts as the positive electrode and the other, graphite, as the negative electrode. The cell is fabricated in the discharged state and on initial charge lithium ions diffuse between the oxygen layers in $LiCoO_2$, pass through the electrolyte and are intercalated between the carbon layers in graphite; discharge reverses this process. Electrons pass around the external circuit. The performance of the battery depends intimately on the solid state chemistry of the electrodes.[2,3] Despite the success of $LiCoO_2$, the development of a future generation of rechargeable lithium-ion batteries is critically dependent on replacing this electrode. The challenge to the solid state chemist is to design and synthesise new lithium transition metal oxides which can fulfil the criteria listed in Table 1 and will in particular possess a lower cost and toxicity than $LiCoO_2$ combined with a higher capacity to cycle lithium ($LiCoO_2$ can only be cycled between $Li_{0.5}CoO_2$ and $LiCoO_2$, corresponding to a capacity of 130 mAh g^{-1}).[3,4] The low cost and toxicity of lithium manganese oxides demand that attention is focused on these. $LiMn_2O_4$ spinel has already been investigated extensively but can only store 110 mAh g^{-1} of charge on cycling.[5–8] Compounds with the formula $LiMnO_2$ would be ideal, provided most of the lithium could be removed and reinserted since this corresponds to a capacity of 285 mAh g^{-1}.

Conventional shake-and-bake methods of solid state synthesis yield a $LiMnO_2$ compound with an orthorhombic symmetry and although electrochemically active the capacity

Table 1 Requirements for a positive electrode material

1	must be an intercalation host for lithium
2	sustain high rates of lithium intercalation and deintercalation→high cell discharge–charge rates
3	highly reversible lithium intercalation→many charge–discharge cycles
4	low Fermi level→high open circuit voltage
5	potential invariant with lithium content→cell potential invariant with state of charge
6	capable of accommodating large quantities of lithium per formula unit→high capacity
7	low formula weight→high gravimetric energy density
8	low molar volume→high volumetric energy density
9	avoid co-intercalation of solvent
10	stable in contact with candidate electrolytes
11	adequate electronic conductivity
12	low cost
13	easily fabricated into composite cathode
14	environmentally friendly

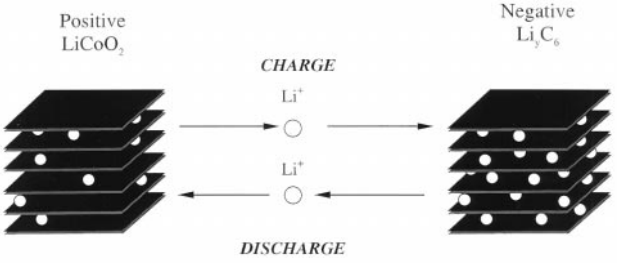

Fig. 1 Schematic representation of a lithium-ion cell.

†Basis of the presentation given at Materials Chemistry Discussion No. 1, 24–26 September 1998, ICMCB, University of Bordeaux, France.

fade on cycling has been found by some authors to be less than ideal.[9,10] The problem we are presented with is to design and synthesise compounds with new structures but the same ($LiMnO_2$) composition. This requires the use of low temperature, *chimie douce*, methods. Ion exchange is an important tool in the low temperature synthesis of solids and it has already been employed to prepare a low temperature orthorhombic $LiMnO_2$ phase by exchanging protons in MnOOH for Li.[11,12] Exchange of Na for Li has been used to prepare $Na_{0.44}MnO_2$ which possesses a complex tunnel structure capable of sustaining high currents (0.5 mA cm^{-2}) and with no perceptible loss of capacity after 100 cycles.[13] Evidently ion exchange has much to offer us when preparing new cathodes.

Synthesis of layered $LiMnO_2$ has been an important target in intercalation chemistry relating to lithium batteries for a number of years.[14] Here again the difficulty arises because conventional synthesis methods cannot yield a layered compound at this composition. However $NaMnO_2$ does adopt a layered structure and the ion exchange strategy has already been used to prepare layered $LiMnO_2$ in highly crystalline and anhydrous form by first forming the sodium phase and then exchanging Na^+ by Li^+.[15–17] Other important studies have taken place on the synthesis of lithium manganese oxides from aqueous solution and these also demonstrate interesting electrochemical activity.[18–20] It has been shown by us and by others,[15,16,21] that most of the lithium can be removed from this compound; hence we have a $LiMnO_2$ material with a high capacity to deliver lithium which would appear to be of considerable technological interest. However, only approximately half the lithium can be reinserted into this structure and in order to optimise the material for performance in rechargeable lithium batteries more work was needed to understand the structural changes that occur on cycling and to relate these to the intercalation mechanism and the electrochemical performance.

We shall, in the succeeding pages, describe the results of studies on layered $LiMnO_2$ which indicate the nature of the structural changes that occur on removing and reinserting lithium, and their relationship to the electrochemical performance of this compound. The substantial improvement on cycling $LiMnO_2$ doped with Co is also discussed.

Experimental

Layered $LiMnO_2$ was synthesised by the method reported previously.[15] The solid-state precursor, $NaMnO_2$, was first prepared following the method reported by Parant *et al.*[22] A 10% stoichiometric excess of Na_2CO_3 (99.5%, Fisons) was thoroughly mixed with Mn_2O_3 (98%, Alfa), heated at 710 °C under flowing argon for 24 hours then air quenched. Ion exchange was carried out by refluxing $NaMnO_2$ (4 g) for 6–8 h in hexanol containing a large excess of LiBr (20–40 g). After cooling and vacuum filtration, the remaining solid was washed with alcohol and dried at 60 °C.

Once cycled, samples are air sensitive and were handled in a MBRAUN high integrity argon filled glove box. X-Ray diffraction patterns of Li_xMnO_2 materials were collected under Mylar film to exclude air. All X-ray diffraction data were obtained on a Philips X-Pert system operating in Bragg–Brentano geometry with Cu-Kα radiation and a secondary monochromator to minimise fluorescence.

Powder neutron diffraction data were collected on the POLARIS diffractometer at the ISIS pulsed source at the Rutherford Appleton Laboratory. The vanadium sample cans were loaded in an argon filled glove box on site, and sealed with PTFE tape and gasket. Structural refinement was carried out by the Rietveld method using programs based on the Cambridge Crystallographic Subroutine Library at the ISIS facility.[23]

For electrochemical studies, the cathodes were prepared by mixing $LiMnO_2$ with SuperS carbon and Kynar Flex 2801 binder (Elf Atochem; dissolved in THF) in a 85:10:5 weight ratio. The resulting slurry was cast onto Al foil, and spread using the doctor-blade technique. After drying, the cast material was pressed under 2.5 tonnes pressure. Disc-shaped electrodes, 13 mm in diameter, were cut and assembled into three-electrode cells with Li metal for both counter and reference electrodes. Cell assembly was carried out in an argon filled glove-box; a standard electrolyte of 1 molal $LiPF_6$ (Battery Grade, Morita) in 2:1 EC:DMC (Electrolyte Grade, Ferro Corp.) solution was used with glass fibre pads as separators. Larger, two-electrode cells were employed to cycle material for the neutron studies. For these cells, the electrodes were cut into 100 cm^2 squares. Typically the large electrodes had a 1 g mass of active material. After cycling, the electrode material was removed from the Al foil and THF was used to extract the binder.

Electrochemical data were collected using a MacPile II (Biologic). Chemical analysis was performed on a Philips PU9400X atomic absorption spectrometer with lithium concentrations determined by flame emission.

Results

Consideration of the results from structural studies or electrochemical measurements taken in isolation does not provide a satisfactory view of the intercalation process in layered $LiMnO_2$. Only by combining data from X-ray and neutron diffraction studies with cyclic voltammetry, load curves and information on capacity fade, it is possible to offer an interpretation of the behaviour of this complex system. As a result we choose first to present the results then discuss the interpretation in a later section.

X-Ray and neutron powder diffraction

Layered $LiMnO_2$ was prepared and fabricated into a composite electrode as described in the Experimental section. A series of cells was charged at a constant current of 30 μA cm^{-2} thus preparing a range of compositions, Li_xMnO_2. The sequence of powder diffraction patterns obtained as a function of x on the first charge is shown in Fig. 2(a). The powder pattern for $LiMnO_2$ indexes on the monoclinic cell obtained previously.[15] The distortion from the ideal rhombohedral symmetry of the layered compound arises from the presence of the Jahn–Teller active Mn^{3+} ion (high spin d^4). Deintercalation to $Li_{0.5}MnO_2$ yields a simpler powder pattern which may be indexed on a rhombohedral cell, $a=2.877$ Å and $c=14.602$ Å. Loss of the monoclinic distortion is due to oxidation of half the Mn^{3+} to Mn^{4+} thus diluting the concentration of the Jahn–Teller active ion to a level where it is insufficient to distort the lattice. Between $Li_{0.5}MnO_2$ and $LiMnO_2$ there exists a two-phase region composed of the monoclinic $LiMnO_2$ and rhombohedral $Li_{0.5}MnO_2$ compounds. A slight shift in the peaks of the monoclinic phase to higher 2θ is evident in the $Li_{0.75}MnO_2$ composition compared with $LiMnO_2$ indicating that a narrow solid solution range may exist for the monoclinic phase before the onset of the two-phase region. A second two-phase region exists between $x=0$ and 0.5. The Li_0MnO_2 phase may be indexed on a rhombohedral cell ($a=2.860$ Å and $c=13.410$ Å) which is significantly smaller than the cell for the $Li_{0.5}MnO_2$ phase. This phase exists alone at the Li_0MnO_2 composition indicating that all the lithium may be extracted from $LiMnO_2$.

A series of electrochemical cells similar to the above was constructed and fully charged to $x=0$ at 30 μA cm^{-2}. They were then discharged to various values of x at the same current density and powder diffraction data were collected. The results are presented in Fig. 2(b). The structural changes occurring on deintercalation [Fig. 2(a)] and reintercalation [Fig. 2(b)] appear to be in sharp contrast. Insertion of 0.2 Li results in a

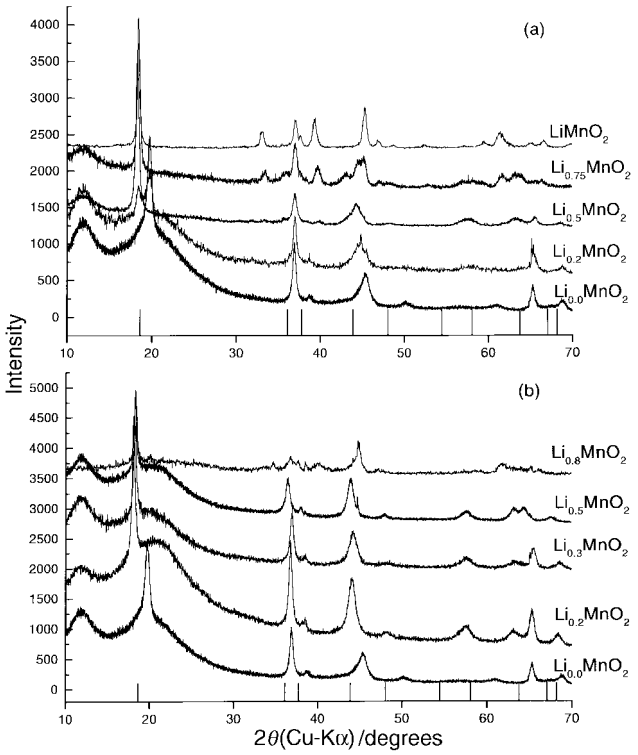

Fig. 2 Powder X-ray diffraction data collected at various values of x for layered Li_xMnO_2 on the first cycle at 30 μA cm^{-2} (a) deintercalation, (b) reintercalation. Vertical lines indicate positions of reflections for $LiMn_2O_4$ spinel. The broad humps at low angles evident in some patterns arise from the other constituents of the composite electrode.

considerable expansion of the c-axis as is evident from the shift to lower 2θ of the lowest angle peak in the pattern. The X-ray powder pattern at this composition is consistent with a single rhombohedral phase. This single phase persists up to at least $Li_{0.5}MnO_2$ with a further slight shift in the lattice parameters to $a=2.8955$ Å, $c=14.5567$ Å. There is no evidence of two crystalline phases. Beyond $Li_{0.5}MnO_2$ the powder X-ray data indicate formation of a monoclinic distortion as expected, given that the Mn^{3+} content is now greater than 50%.

Distinguishing between layered and spinel phases using diffraction data can be problematical because of the similarity that can occur in their powder diffraction patterns. A rhombohedral cell with a c/a ratio of 4.9 is equivalent, geometrically, to a cubic cell. Careful examination of the X-ray data indicates that the peaks in the powder patterns for $x \leqslant 0.5$ could not be adequately described by a spinel model; even allowing for variation in the lattice parameter of spinel, the c/a ratios of the rhombohedral phases are $\neq 4.9$. The breadth of the peaks means that the presence of spinel as a minority phase cannot be ruled out, however the peaks at $x=0.5$ on the first discharge are quite well defined [Fig. 2(b)] and there is little evidence of spinel in this pattern.

To explore further the structural changes on cycling, a large cell was subjected to five cycles at a current density of 100 μA cm^{-2} between potential limits of 2 and 4.6 V. Cycling terminated at the composition $Li_{0.5}MnO_2$ on the sixth charge and neutron data were collected. All attempts to fit the data using only a rhombohedral model proved unsatisfactory. The possibility of a single layered phase with Mn displaced into the Li layers and *vice versa* was also investigated but did not significantly improve the fit. A spinel structure would not fit the data and permitting the manganese ions to disorder within the cubic cell of spinel did not yield a satisfactory fit. A two-phase refinement was investigated using a combination of the layered rhombohedral phase, $Li_{0.5}MnO_2$, and cubic spinel, $LiMn_2O_4$; this provided a satisfactory fit, Fig. 3. Evidently

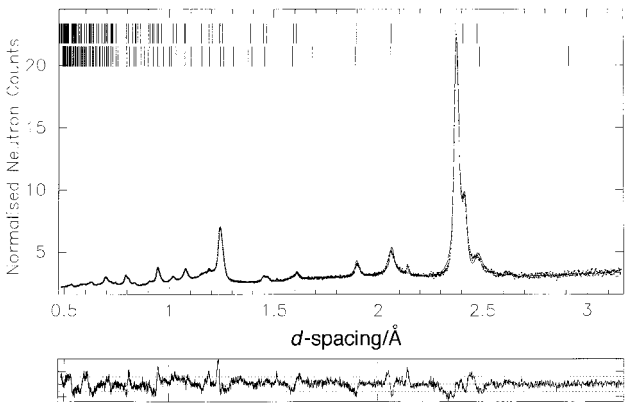

Fig. 3 Powder neutron diffraction data for $Li_{0.5}MnO_2$ after five cycles at 100 μA cm^{-2} within the range 2–4.6 V showing that a two-phase model composed of rhombohedral $Li_{0.5}MnO_2$ and cubic $LiMn_2O_4$ spinel fits the data. Dots represent the observed data, solid line the calculated pattern and the difference/e.s.d. plot is shown at the bottom of the figure.

after 5 cycles there is significant conversion of layered $LiMnO_2$ to spinel.

Electrochemistry

Initial investigation of Li_xMnO_2 was carried out using cyclic voltammetry, Fig. 4. A rate of 10 μV s^{-1} between potential limits of 2 and 4.6 V was employed. Cycling commenced with oxidation from the open circuit potential of 3 V. The most striking feature is the difference between the first and subsequent cycles. In fact the greatest difference is to be found in the low voltage oxidation process: on the first charge the peak is located at 3.6 V but on the second charge a peak appears at 3.25 V. There is also some diminution in the magnitude of the oxidation peak at 4 V. The reduction processes show only a small change on cycling. The load curve for the first charge, collected at 10 μA cm^{-2}, is shown in Fig. 5, from which two plateaux may be identified corresponding to the two oxidation processes in Fig. 4. The variation of capacity with cycle number at two different current densities is shown in Fig. 6. At 100 μA cm^{-2}, the first charge is associated with a specific capacity of 220 mAh g^{-1} but this falls significantly to only 130 mAh g^{-1} on the subsequent discharge. Thereafter, the capacity on charge and discharge is very similar at around 130 mAh g^{-1}. This is in accord with the CV in Fig. 4 and reinforces the view that the electrochemical evidence points to a change occurring during the first charge. At the high current density of 1 mA cm^{-2} the specific capacity on the first charge is now 180 mAh g^{-1}, dropping to 90 mAh g^{-1} on the sub-

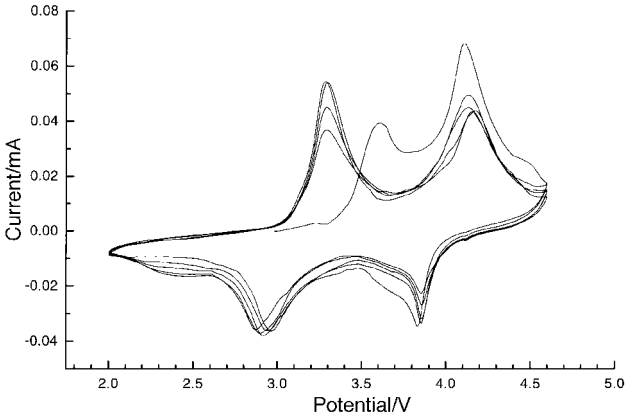

Fig. 4 Cyclic voltammogram of layered $LiMnO_2$ including five cycles at 10 μV s^{-1} within the range 2–4.6 V *vs.* Li^+(1 M)/Li couple. The first cycle is markedly different on charge than subsequent cycles.

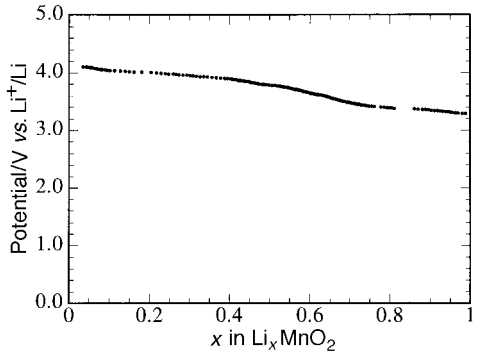

Fig. 5 Variation of potential with composition, x, Li_xMnO_2, on charging at 10 μA cm^{-2}.

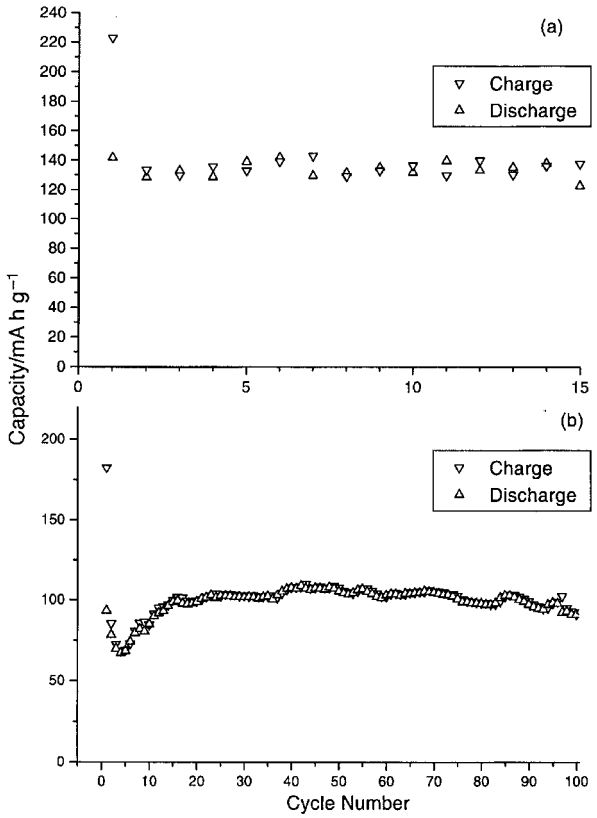

Fig. 6 Variation of specific capacity with the number of cycles for layered $LiMnO_2$ at (a) 100 μA cm^{-2} and 2.0–4.6 V, (b) 1 mA cm^{-2} and 2.6–4.6 V.

sequent charge. Thereafter, there is a further drop in the capacity which reaches a minimum after five cycles and then recovers to a plateau at 100 mAh g^{-1} after some 15–20 cycles.

The load curve on cycling is presented in Fig. 7 along with that of spinel. The curves are clearly very different, however the two plateaux on discharge for $LiMnO_2$ do occur at broadly similar potentials to the 3 and 4 V plateaux of spinel. These results support the proposition that layered $LiMnO_2$ converts to a spinel phase on cycling.

Discussion

Neutron diffraction has demonstrated the presence of cubic spinel after 5 cycles, however, there appears to be little evidence of conversion to spinel within the first cycle, as indicated by X-ray diffraction. In apparent contrast, the electrochemical results change not just within the first cycle but on the first charge, Fig. 4; thereafter the CV's alter little on passing

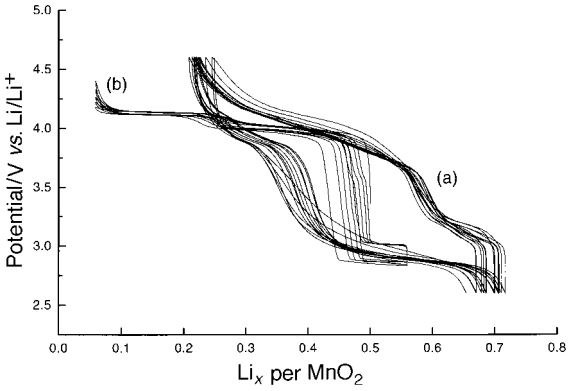

Fig. 7 Variation of potential with composition on cycling at a current density of 100 μA cm^{-2} and 2.6–4.6 V for (a) layered $LiMnO_2$ and (b) $LiMn_2O_4$ starting from the third cycle. Compositions are expressed in terms of Li_xMnO_2.

through the 5th cycle. We propose the following model as a possible rationalisation of these apparently contradictory facts.

On removing lithium from layered $LiMnO_2$ the cooperative, static, Jahn–Teller distortion becomes unstable and segregation of Li^+ ions and electrons occurs within the particles, forming lithium deficient regions of composition $Li_{0.5}MnO_2$. These occupy a shell near the surface of the particles with a lithium rich $LiMnO_2$ region of monoclinic symmetry near the core. This core–shell model persists for compositions in the range $0.5 < x < 1$ where deintercalation involves movement of the phase boundary between the rhombohedral and monoclinic regions. This process is associated with the peak in the cyclic voltammogram at around 3.6 V on the first charge.

Layered $Li_{0.5}MnO_2$ has the ideal spinel composition, $LiMn_2O_4$, and furthermore the spinel structure may be easily derived from layered $Li_{0.5}MnO_2$ by displacing one quarter of the manganese ions from the transition metal layers into empty octahedral sites in the lithium layers. Displacement of V ions from the transition metal to the lithium layers has been observed in the structurally similar layered compound $LiVO_2$, upon extraction of lithium.[24] The presence of $Mn^{4+/3+}$ ions in the lithium layers will result in displacement of Li^+ ions from their octahedral sites, which share edges with the $Mn^{4+/3+}$ octahedra, into tetrahedral sites with which the Mn sites share only corners. In this way the Li^+–$Mn^{4+/3+}$ repulsions will be minimised. As a result of the Li and Mn displacements small regions with the local structure and composition of spinel will be formed. Whether this occurs at the $Li_{0.5}MnO_2$ composition or whether it is triggered only when the lithium content is reduced below $Li_{0.5}MnO_2$ is as yet unknown. Further lithium extraction will involve removal of Li^+ from the tetrahedral sites.

The voltages at which peaks occur in cyclic voltammograms correspond to the energetics of the intercalation process, specifically the energies of the lithium ions in their sites and the electrons. Intercalation involving the tetrahedral sites in $LiMn_2O_4$ spinel occurs at 4 V. The site energies are determined, to a first approximation, by the local environment and will be the same in regions with the local structure of spinel as they are in large crystals. The model presented above proposes the formation of tetrahedrally coordinated Li^+ ions in a local spinel-like environment at $Li_{0.5}MnO_2$ which in turn explains the presence of the 4 V peak in the CV's on the first charge, Fig. 4. The validity of the model is further reinforced by the fact that the position of the 4 V peak in the CV's is invariant up to and beyond the 5th cycle at which point the neutron diffraction data show clear evidence of spinel.

Despite local structure elements which resemble spinel, the average crystal structure will remain essentially layered after one cycle, as observed in the X-ray data. We propose that

subsequent cycling results in consolidation of the spinel structure until, after five cycles, long range ordered spinel emerges, as is evident in Fig. 3. A related model has been proposed by Vifins and West,[21] although in that case the transformation to spinel is believed to occur mainly on the reinsertion of lithium at deep discharge (low voltages). We believe the similarity of the 4 V peak on the first and subsequent charges implies that the formation of spinel like regions is triggered by the first deintercalation.

Recently we have carried out HREM studies of layered $LiMnO_2$ as a function of lithium cycling. The results are reported in detail elsewhere.[25] The conclusions pertinent to the present paper are that the proportion of the spinel phase increases on cycling and there is direct evidence for a complex microstructure in which spinel-like regions are embedded in layered material, supporting the model proposed here.

The load curve for layered $LiMnO_2$, Fig. 7, deserves further comment. The data correspond to cycles for which the diffraction patterns show evidence of spinel and layered phases. The curve resembles a hysteresis loop for a ferroelectric material where such hysteresis arises from domain wall motion, as is well documented. The similarity here is that we also have a heterogeneous system with a complex microstructure (involves both the layered and spinel regions), although there is a difference between this and the ferroelectric case in that here there is compositional inhomogeneity. The origin of the hysteresis in this case may be found in the need to move phase boundaries between compositionally distinct regions as lithium ions are inserted and removed from the host structure. Hysteresis has been observed in load curves previously by McKinnon *et al.*[26] although in general it has been ignored.

Experience tells us that the cubic spinel $LiMn_2O_4$ has proved to be far more complex than was originally thought when it was introduced as an intercalation host in 1983.[27,28] It appears that the layered compound demonstrates at least as much richness in its intercalation chemistry and that further analysis will be required in order to understand fully the details of the electrochemical process.

$Li(Mn_{1-y}Co_y)O_2$

Although the intercalation chemistry of $LiMnO_2$ is scientifically interesting, the loss of capacity on the first cycle renders an otherwise promising material of less interest technologically. The challenge is to modify $LiMnO_2$ in order to improve substantially the capacity retention on cycling. This we have done by replacing a small amount of the Mn^{3+} by Co^{3+}. The results of this study are reported elsewhere but are summarised here to provide a more complete picture of the layered $LiMnO_2$ based system.[29]

A range of compositions, $Li(Mn_{1-y}Co_y)O_2$ where $0<y<0.5$, has been synthesised by first preparing the mixed metal sodium phase then ion exchanging for lithium as described above. The optimum cycling performance was obtained for the material containing 10% Co and hence attention will be focused on this composition. The compound as prepared is slightly lithium deficient, $Li_{0.85}(Mn_{0.9}Co_{0.1})O_2$. Composite cathodes were fabricated as for the $LiMnO_2$ material and the cycling curve is shown in Fig. 8. The data were collected at $100\ \mu A\ cm^{-2}$ over the potential range of 2.6–4.85 V. The initial capacity is comparable to $LiMnO_2$ but the capacity retention is dramatically improved compared with the pure Mn material, with capacities of *ca.* 200 mAh g^{-1} after 20 cycles. X-Ray (Fig. 9) and neutron diffraction data collected for the as-prepared 10% Co compound may be indexed on a rhombohedral unit cell with lattice parameters $a=2.8750(2)$ Å and $c=14.3930(8)$ Å, and there is no evidence of a monoclinic distortion arising from the Jahn–Teller active Mn^{3+} ion. Profile refinement by the Rietveld method confirms that the compound

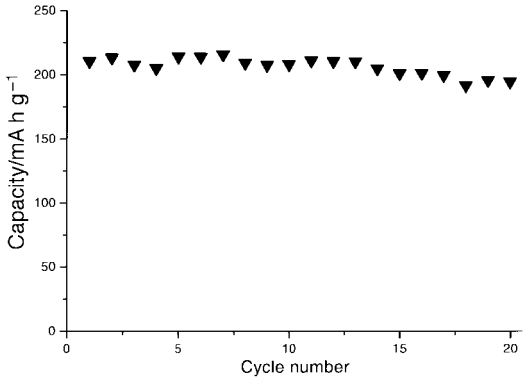

Fig. 8 Specific discharge capacity as a function of cycle number for layered $Li(Mn_{0.9}Co_{0.1})O_2$ at $100\ \mu A\ cm^{-2}$ and 2.6–4.8 V.

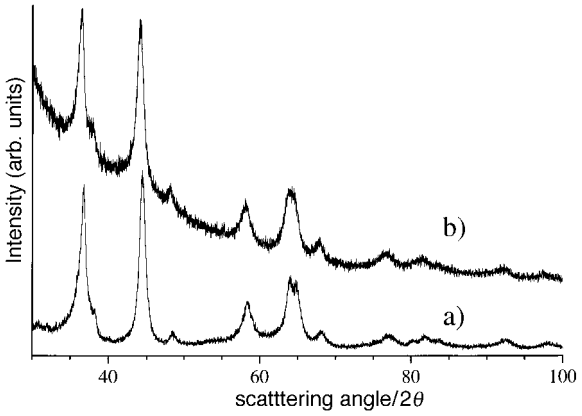

Fig. 9 Powder X-ray diffraction data for $Li(Mn_{0.9}Co_{0.1})O_2$ (a) before and (b) at the end of the discharge after four cycles at $100\ \mu A\ cm^{-2}$ and 2.6–4.85 V.

is isostructural with $LiCoO_2$ and that the Mn : Co ratio is close to 9 : 1. We have intercalated 0.15 lithiums forming the $Li(Mn_{0.9}Co_{0.1})O_2$ composition and still there is no evidence of a distortion. Cobalt may be in the 2+ or 3+ oxidation state. The latter would imply that 90% of the transition metal sites were occupied by Mn^{3+} while the former would imply 80% occupancy. In either case it is surprising that the Jahn–Teller distortion is absent. An understanding of why this is so must await the results of further studies currently underway. The lack of a Jahn–Teller distortion persists on cycling, Fig. 9, and may, at least in part, be responsible for the improved capacity retention.

P.G.B. is indebted to the EPSRC, the EU (Esprit programme) and to NEDO for financial support.

References

1 B. Scrosati, *Nature*, 1995, **373**, 557.
2 *Solid State Electrochemistry*, ed. P. G. Bruce, Cambridge University Press, Cambridge, 1995.
3 P. G. Bruce, *Chem. Commun.*, 1997, 1817.
4 P. G. Bruce, *Philos. Trans. R. Soc. London A*, 1996, **354**, 1577.
5 (*a*) R. J. Gummow, A. de Kock and M. M. Thackeray, *Solid State Ionics*, 1994, **69**, 59; (*b*) J. M. Tarascon, W. R. McKinnon, F. Coowar, T. N. Bowmer, G. Amatucci and D. Guyomard, *J. Electrochem. Soc.*, 1994, **141**, 1421; J. M. Tarascon, F. Coowar, G. Amatucci, F. K. Shokoohi and D. G. Guyomard, *J. Power Sources*, 1995, **54**, 103.
6 H. Huang and P. G. Bruce, *J. Electrochem. Soc.*, 1994, **141**, L106.
7 H. Huang and P. G. Bruce, *J. Power Sources*, 1995, **54**, 52.
8 Japan Electronics, March 6th, 1996.
9 L. Crogvennec, P. Deniard, R. Brec and A. Lecerf, *J. Mater. Chem.*, 1997, **7**, 511.

10 Zx. Shu, I. J. Davidson, R. S. McMillan and J. J. Murray, *J. Power Sources*, 1997, **68**, 618.
11 J. M. Reimens, E. Fuller, E. Rossen and J. R. Dahn, *J. Electrochem. Soc.*, 1993, **140**, 3396.
12 I. Koetschou, M. N. Richard, J. R. Dahn, J. B. Soupart and J. C. Rousche, *J. Electrochem. Soc.*, 1995, **142**, 2906.
13 A. R. Armstrong, H. Huang, R. A. Jennings and P. G. Bruce, *J. Mater. Chem.*, 1998, **8**, 255.
14 M. M. Thackeray, *J. Electrochem. Soc*., 1995, **142**, 2558.
15 A. R. Armstrong and P. G. Bruce, *Nature*, 1996, **381**, 499.
16 F. Capitaine, P. Gravereau and C. Delmas, *Solid State Ionics*, 1996, **89**, 197.
17 C. Delmas and F. Capitaine, Presented at the *8th Int. Meeting on Lithium Batteries*, Nagoya, Japan, 1996.
18 F. Leroux, D. Guyomard and Y. Piffard, *Solid State Ionics*, 1995, **80**, 299.
19 F. Leroux, D. Guyomard and Y. Piffard, *Solid State Ionics*, 1995, **80**, 307.
20 L. Sánchez and J.-P. Pereira-Ramas, *Electrochim. Acta*, 1997, **42**, 531.
21 G. Vitins and K. West, *J. Electrochem. Soc.*, 1997, **144**, 2587.
22 J. P. Parant, R. Olazcuaga, M. Devalette, C. Fouassier and P. Hagenmuller, *J. Solid State Chem.*, 1971, **3**, 1.
23 J. C. Matthewman, P. Thompson and P. J. Brown, *J. Appl. Crystallogr.*, 1982, **15**, 167.
24 M. M. Thackeray, L. A. de Picciotto, W. I. F. David, P. G. Bruce and J. B. Goodenough, *J. Solid State Chem.*, 1987, **67**, 285.
25 J. Shao-Horn, S. A. Hackney, A. R. Armstrong, P. G. Bruce, R. L. Gitzendanner, C. S. Johnson and M. M. Thackeray, *J. Electrochem. Soc.*, submitted.
26 W. R. McKinnon, *Solid State Electrochemistry*, ed. P. G. Bruce, Cambridge University Press, 1995, ch. 7.
27 M. M. Thackeray, W. I. F. David, P. G. Bruce and J. B. Goodenough, *Mater. Res. Bull.*, 1983, **18**, 461.
28 M. M. Thackeray, P. J. Johnson, L. A. de Picciotto, W. I. F. David, P. G. Bruce and J. B. Goodenough, *Mater. Res. Bull.*, 1984, **19**, 179.
29 A. R. Armstrong, R. Gitzendanner, A. D. Robertson and P. G. Bruce, *Chem. Commun.*, 1998, 1833.

Paper 8/03938K